Gas-Phase Stability of Tetrahedral Multiply Charged Anions: A Conceptual and Computational DFT Study

Goedele Roos, Frank De Proft, and Paul Geerlings*

Vrije Universiteit Brussel (VUB), Algemene Chemie (ALGC), Pleinlaan 2, B-1050, Brussels, Belgium

Received: August 23, 2004; In Final Form: November 6, 2004

Multiply charged anions (MCA's) are unstable relative to electron autoejection; however, the repulsive Coulomb barrier (RCB) provides electronic stability. In view of their interest in biological systems, the behavior of isolated AsO_4^{3-}, PO_4^{3-}, SO_4^{2-}, and SeO_4^{2-} in the gas phase and in solution has been studied. To calculate the RCB values, the electrostatic and point charge model—two methods currently used in the literature—are applied, together with a recently introduced Conceptual Density Functional Theory (DFT) based approach. The relative stability of the above-mentioned MCA's is compared. The trends of the RCB are analyzed by including analogous compounds from the second and third row and by passing from dianionic to trianionic systems. Considering the effect of solvent, using the SCI-PCM solvent model, the evolution of the RCB when passing to higher dielectric constants is evaluated. The RCB is related to the properties of the system as polarizability/softness. Both a numerical and a conceptual correlation between the RCB and the global softness is found.

Introduction

Multiply charged anions (MCA's) are common in the condensed phase and play an important role in chemistry, material science, and biochemistry. Many familiar inorganic MCA's in the gas phase are for example present as stable entities in proteins, where they are stabilized with respect to electron emission through the numerous interactions with the enzymatic environment. An example recently studied by our group[1] is the stabilization of the negative charge of the dianionic substrate arsenate complexed to the enzyme arsenate reductase (ArsC). Upon binding, due to the several ArsC−arsenate hydrogen bonds, negative charge from arsenate is transferred to ArsC by which the dianionic arsenate passes into an intermediate form between the mono- and dianion. Phosphates, sulfates, and selenates are other examples of inorganic compounds that are present as stable multiply charged species in proteins such as phosphatases, sulfate-binding protein, and molybdenum enzyme.[2]

In the gas phase, however, one has to deal with the "electronic" instability of MCA's. The strong intramolecular Coulomb repulsion due to the excess of negative charge makes MCA's very fragile and sensitive to electron autodetachment.[3] Therefore, MCA's have rarely been observed in the gas phase until very recently, when increasingly sophisticated experimental tools based on photoelectron spectroscopy (PES) and electrospray ionization have become available.[3,4]

The experimental observation of MCA's can be explained by the existence of a repulsive Coulomb barrier (RCB) hindering the emission of one of the excess electrons. Starting from an *N*-electron reference system with charge *n*, the escaping electron experiences both a valence-range attractive potential that acts to bind the electron and a long-range Coulomb repulsive potential caused by the remaining $(n - 1)$-charged anion. If in the valence region the attractive valence potentials are stronger than the repulsive Coulomb potentials, the lowest bound state of the *n*-charged anion lies below the lowest state of the $(n - 1)$-charged anion, and the *n*-charged anion is electronically stable. On the other hand, when the Coulomb repulsive potential is strong enough to outweigh the attractive potentials, the *n*-charged anion is electronically unstable with respect to the $(n - 1)$-charged anion. However, the existence of the RCB stabilizes the *N*-anion through which a metastable anion of charge *n* results[5] (Figure 1). The RCB requires the departing electron to overcome a potential barrier to escape, which can be a very unlikely process. Consequently, relatively long but finite lifetimes can be observed for metastable species.[5−7]

Since arsenate, phosphate, selenate, and sulfate are of biological interest, these MCA's are often target for theoretical studies of enzymatic processes.[8,9] Consequently, it is of fundamental chemical and physical significance to understand the behavior of these MCA's in the gas phase.

The increase of computational power during the last few decades has allowed us to perform detailed theoretical studies on realistic enzymatic systems. A combination of these theoretical studies and well-established experimental investigations (structural investigations, pH rate profiles, kinetic isotope effects, ...) provides a better understanding and more precise information on both structural and kinetic aspects of enzyme action. However, due to their size, quantum-theoretical investigations of biosystems still call for the use of model systems, in which stabilizing interactions of the environment are often reduced or sometimes left out to ensure high computation accuracy, the most extreme case being the isolated species in the gas phase.

In the present study, RCB's are calculated for trianionic arsenate (AsO_4^{3-}) and phosphate (PO_4^{3-}) and dianionic sulfate (SO_4^{2-}) and selenate (SeO_4^{2-}). Two methods currently used in the literature are applied: the electrostatic[10] and the point charge (PCM)[6,7] model. A third approach, based on Conceptual Density Functional Theory (DFT),[11] including the softness, Fukui function, ... of the $(n - 1)$-charged system, is introduced to calculate the RCB.

* Corresponding author. Phone: +32-2-629-33-14. Fax: +32-2-629-33-17. E-mail: pgeerlin@vub.ac.be.
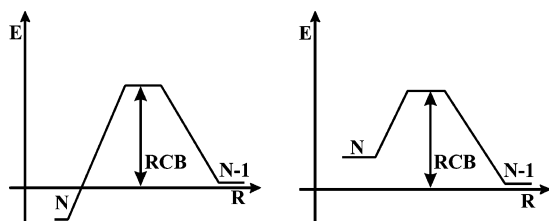
GP Stability of Tetrahedral Multiply Charged Anions

J. Phys. Chem. A, Vol. 109, No. 4, 2005 **653**

Figure 1. Schematic potential energy curves showing both the binding energy of an electron to a $(n - 1)$-charged system as well as the repulsive Coulomb barrier (RCB). (A) Original n charged N-electronic system is stable; (B) N-electronic system is metastable. $R =$ the distance to the ejected electron.

The relative stability of the mentioned MCA's toward each other is compared and the question is addressed how to relate the RCB to the nature of the studied systems. The trends of the RCB are analyzed by including analogous compounds from the second and third row and by passing from dianionic to trianionic systems. Since the studied anions are highly polarizable, the relationship between the trends in the RCB values and the trends in the global softness (S)[12] is explored.

Also, the stabilizing effect of solvent on MCA's is investigated.

Theoretical Background

Although the RCB is clearly dominated by the electrostatic interaction between the outgoing electron and the residual anion, it is emerging from a nonlocal and energy-dependent potential.[6,7] An exact theory for the RCB can be derived in the framework of Green's function theory, in analogy to scattering potentials, to which the RCB is closely related. The Green's function (GF) obeys a Dyson equation, relating the GF for the total system to the free GF's of the unperturbed anion via its self-energy. The self-energy corresponds to the exact potential experienced by an electron when it is emitted from the electronically unstable MCA, and can thus be identified with the RCB. The exact self-energy is not straightforward to compute, and due to its nonlocal, energy-dependent, and probably complex nature not easily depictable.[6,7] Therefore, approximations have to be made.

Simons et al. have shown that a simple Coulomb-energy model can be applied to roughly estimate the height of the RCB of compact stable and metastable MCA's.[5]

Beyond this simple Coulomb model, the RCB can be computed in the framework of local ab initio approaches, which are meaningful approximations for the true RCB, when the system under investigation is spatially extended.[6]

A straightforward and natural way to estimate the RCB is to compute the total energy of the $(N - 1)$-system in the presence of a negative point charge, which may represent the outgoing electron. If the negative point charge is placed at varying distances r to the monoanion, one readily obtains a complete potential barrier profile. The RCB determined by the point charge model (PCM) potential, denoted as $V_{PCM}(\mathbf{r})$, is then obtained from the equation

$$V_{PCM}(\mathbf{r}) = E_0(\mathbf{r}) - E_0 \quad (1)$$

with $E_0(r)$ being the total energy of the $(N - 1)$-system in the presence of the negative point charge at position $\mathbf{r}$, while E_0 is the total energy of the $(N - 1)$-system.[6,7]

Note that when using atomic units, the charge of an electron (absolute value) equals 1, so energy and potential are numerically equal here and will be used together throughout.

The point charge model correctly describes the remaining $(N - 1)$-anion at large distances between the point charge and the remaining $(N - 1)$-anion, but possesses some weakness at short distances. By fixing the approaching electron at a certain position $\mathbf{r}$ through which this electron becomes distinguishable from the other $N - 1$ electrons of the system, the PCM model loses accuracy. When the electron approaches, the $(N - 1)$-system becomes statically polarized. This can only happen when the electron approaches with high velocity. Because this is not necessarily the case, the static polarization of the $(N - 1)$-system makes the PCM model less rigorous. (For an extensive discussion see refs 6 and 7.)

The electrostatic model[10] calculates the RCB as the potential energy of interaction between an electron and a charged sphere. This potential energy is largely governed by the polarization and the long-range Coulomb repulsion and is given by

$$W = -\frac{14.4}{2}\frac{\alpha}{R^4} + Q\frac{14.4}{R} \quad (2)$$

Equation 2 is the generalization of eq 1 of ref 11 and gives the case of a multiply charged sphere, α is the polarizability (in $Å^3$), Q (in au) is the remaining charge of the sphere after the electron has left, and R (in Å) is the distance between the center of mass of the charged sphere and the leaving electron. The conversion factor 14.4 is given in eV Å.

Within the framework of Conceptual DFT,[11] our group proposed a methodology to calculate the interaction energy between a molecule and a single point charge, based on first-order perturbation theory to the electron density.[13] This method was originally used to calculate interaction energies in adsorption processes of zeolites[13] and is applied in this work for the first time to calculate RCB's.

The interaction energy $\Delta E(\mathbf{R})$ of a molecule and a single point charge q is given by

$$\Delta E(\mathbf{R}) = qV(\mathbf{R}) + q^2 \int \int \frac{\omega(\mathbf{r},\mathbf{r}')}{|\mathbf{r} - \mathbf{R}||\mathbf{r}' - \mathbf{R}|} \, d\mathbf{r} \, d\mathbf{r}' = \\ \Delta E_1(\mathbf{R}) + \Delta E_2(\mathbf{R}) \quad (3)$$

where $V(\mathbf{R})$ can be identified as the classical molecular electrostatic potential (MEP)[14] at position R. In a point charge model and for molecules at large distances, the first term of eq 3 reduces to the Coulomb term of eq 2.

$\omega(\mathbf{r},\mathbf{r}')$ stands for the linear response function $(\{\partial\rho(\mathbf{r})\}/\{\partial v(\mathbf{r}')\})_N$. According to the Berkowitz−Parr relation,[15] $\omega(\mathbf{r},\mathbf{r}')$ is equal to

$$\omega(\mathbf{r},\mathbf{r}') = \frac{s(\mathbf{r})s(\mathbf{r}')}{S} - s(\mathbf{r},\mathbf{r}') \quad (4)$$

$\Delta E_2(\mathbf{R})$ includes the response of the system's density to the change in potential due to the leaving electron as seen from its exact expression for $\Delta E_2(\mathbf{R})$

$$\Delta E_2(\mathbf{R}) = \int \int \omega(\mathbf{r},\mathbf{r}')\delta v(\mathbf{r}')\delta v(\mathbf{r}) \, d\mathbf{r} \, d\mathbf{r}' \quad (5)$$

where $\delta v(\mathbf{r})$ stands for a variation in the external (i.e. due to the nuclei and, in the MCA case, the leaving electron) potential. Writing the external potential due to the leaving electron as

$$\Delta v(\mathbf{r}) = -\frac{1}{|\mathbf{r} - \mathbf{R}|} \quad (6)$$

and $s(\mathbf{r},\mathbf{r}')$ as usual simplified to[16]

$$s(\mathbf{r},\mathbf{r}') \approx Sf(\mathbf{r})\delta(\mathbf{r} - \mathbf{r}') \qquad (7)$$

where $f(\mathbf{r})$ is the electronic Fukui function and S the global softness, $\Delta E_2(\mathbf{R})$ can be written as[13]

$$\Delta E_2(\mathbf{R}) \approx S\left(\left(\frac{\partial Vel(\mathbf{R})}{\partial N}\right)_v^2 - \int \frac{f(\mathbf{r})}{|\mathbf{r} - \mathbf{R}|^2}\, d\mathbf{r}\right) \qquad (8)$$

This term is a correction term arising from the change in electron density of the MCA when the excess electron is emitted and involves besides global properties, such as the global softness (S), also two local properties: the N-derivative of the electronic part of the electrostatic potential ($\{\partial Vel(\mathbf{R})\}/\{\partial N\})_v$ and the electronic Fukui function $f(\mathbf{r}) = (\{\partial\rho(\mathbf{r})\}/\{\partial N\})_v$, being the N-derivative of the electron density function, both evaluated at constant external potential.

For a wave function obeying the Hellmann–Feynman theorem, $\int\{f(\mathbf{r})\}/\{|\mathbf{r} - \mathbf{R}|^2\}\, d\mathbf{r}$ is the nuclear Fukui function[17] $\Phi(\mathbf{R})$ and can be written as $|(\{\partial F(\mathbf{R})\}/\{\partial N\})_v|$ where $F(\mathbf{R})$ is the force due to the electronic Fukui function acting on a unit charge placed at $\mathbf{R}$.

The response of the $(N - 1)$-system's density to the departing electron is fully included into the PCM model,[7] while an additional approximation (eq 7) has to be made on eq 5, itself derived from first-order perturbation theory, to obtain the working eq 8. Therefore, the DFT based expression can be considered as less exact in comparison to the PCM model, but has the advantage of being expressed in terms of molecular reactivity descriptors, describing the evolution of a system when passing from $N - 1$ to N electrons and vice versa.

$\Delta E_2(\mathbf{R})$ explicitly demonstrates a dependence on S, which was seen to be proportional to α,[16,18] yielding a correspondence with the R^{-4} term in eq 2.

Computational Details

Calculations were performed on AsO_4^{3-}, PO_4^{3-}, SO_4^{2-}, and SeO_4^{2-}. The geometries of the considered N-charged anions were optimized by using the B3LYP[19] exchange-correlation functional with a 6-31+G** basis set.[20] All further calculations were carried out on these optimized geometries at the B3LYP/6-31+G** level. To ensure a constant external potential needed in the calculation of the DFT descriptors, calculations on the $(n - 1)$-charged systems were also performed on the optimized geometries of the n-charged systems.

The polarizability α appearing in eq 8 was calculated as the arithmetic average of the diagonal elements of the polarizability tensor

$$\alpha = (\alpha_{xx} + \alpha_{yy} + \alpha_{zz})/3 \qquad (9)$$

obtained analytically.

The global softness S present in eq 3 is given by the finite difference approximation

$$S \approx \frac{1}{I - A} \qquad (10)$$

where I and A are the ionization energy and the electron affinity, respectively.

In eq 10, the ionization energy (I) and the electron affinity (A) are set equal to zero when negative values are found. Consequently, for SO_4^{2-} and SeO_4^{2-}, S is approximated by the inverse of the ionization energy while for PO_4^{3-} and AsO_4^{3-} S is undefined (both I and A are negative). To overcome this problem, the equality of the ratio of the global softness of the
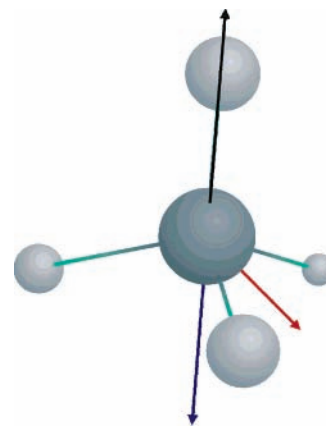

Figure 2. Directions into which potential curves for electron emission are calculated for the tetrahedral anions $XO_4^{2-/3-}$ with X = S, Se, As, and P. Color code: threefold axis, X–O (positive direction), black; threefold axis, O–X (negative direction), blue; twofold axis, O–Y (Y is the midpoint between two oxygen atoms), red.

TABLE 1: Calculated (B3LYP/6-31+G) Ionization (I) and HOMO (ϵ_{HOMO}) Energies (au) of SO_4^{2-}, SeO_4^{2-}, AsO_4^{3-}, and PO_4^{3-}**

	I	ϵ_{HOMO}
SO_4^{2-}	−0.0478	0.132
SeO_4^{2-}	−0.0247	0.105
PO_4^{3-}	−0.2636	0.332
AsO_4^{3-}	−0.2357	0.298

$(N - 1)$-system and the $(N - 2)$-system (S_{N-1} and S_{N-2}, respectively) with the ratio of their polarizabilities (α_{N-1} and α_{N-2}) is used

$$\frac{S_{N-1}}{S_{N-2}} \approx \frac{\alpha_{N-1}}{\alpha_{N-2}} \qquad (11)$$

This equality is based on the proposed proportionality between S and α.[16,18]

($\{\partial Vel(\mathbf{R})\}/\{\partial N\})_v$ and $|(\{\partial F(\mathbf{R})\}/\{\partial N\})_v|$ are calculated by using the finite difference approach in which ΔN is set equal to 1.

The electrostatic model yields a spherically averaged potential, while both the PCM model and the DFT based model provide direction-dependent potentials. As a consequence, when using the PCM model and the DFT-based model, potential curves for electron emission can be obtained for all possible directions. For the tetrahedral anions considered here, the RCB was calculated into the positive and negative direction of one of the four equivalent 3-fold X–O axes (X = As, P, S, Se) and in the direction of one of the two equivalent 2-fold X–Y axes (with Y the midpoint between two oxygen atoms) (Figure 2).

To investigate the stabilization of MCA's in solvent, the SCI-PCM[21] solvent model was used.

All calculations were performed with the GAUSSIAN 03[22] package.

Results and Discussion

Electronically Unstable MCA's. The electronic instability of AsO_4^{3-}, PO_4^{3-}, SO_4^{2-}, and SeO_4^{2-} can be seen through both their positive HOMO energies found in agreement with ref 23 (Table 1) and their negative ionization energies, implying that the anion A^{n-} at its optimal geometry has a higher energy than the corresponding anion $A^{(n-1)-}$ with lower charge at the same geometry.

GP Stability of Tetrahedral Multiply Charged Anions

J. Phys. Chem. A, Vol. 109, No. 4, 2005 **655**

TABLE 2: RCB's (eV) Calculated (B3LYP/6-31+G**) with the Electrostatic (Eq 2), the PCM (Eq 1), and the DFT Based (eqs 3 and 8, with S calculated with eq 10, see discussion) Models Compared with the Global Softness S (au, calculated with eq 14) of the $(n-1)$-Charged System

	RCB electrostatic model	RCB PCM	RCB DFT based model	$S(n-1)$
SO_4^{2-}	3.62	3.85	11.81	16.18
SeO_4^{2-}	3.07	3.40	10.69	17.57
PO_4^{3-}	8.25	8.28	25.79	17.09
AsO_4^{3-}	7.37	7.79	25.14	18.49

Calculation of the RCB. As mentioned before, the existence of the RCB stabilizes the MCA's through which these MCA's receive a metastable nature.[6,7] The RCB's calculated with the PCM model[6,7] (eq 1), the electrostatic model[9] (eq 2), and the DFT-based approach (eqs 3 and 8) are given in Table 2 and Figure 3.

The RCB values calculated with the electrostatic and the PCM model are of comparable magnitude. The values calculated with the DFT model are about three times larger than the other estimations of the RCB, but qualitatively, the three calculation methods for the RCB give similar results. From the graphs presented in Figure 3, it is seen that when the barrier height decreases, the position of the barrier is slightly shifted to a longer distance from the nucleus. The RCB values obtained for the dianionic systems are considerably lower than those for the trianionic systems. This is in agreement with the statement by Dreuw and Cederbaum[6,7] that the magnitude of the RCB strongly depends on the electrostatic repulsion between the excess negative charge and the escaping electron. Therefore, higher negatively charged species, e.g., trianions, in general give rise to higher repulsive Coulomb barriers than less charged species, e.g., dianions. For a given ionic charge, the RCB values decrease when the global softness S of the considered systems increases.

The direction dependence of the RCB can be studied with the PCM model and DFT based models, because these models provide direction-dependent potentials. It appears that the difference in molecular environment experienced by the electron emitted along the different directions shown in Figure 2 is relatively small when the PCM model is used. A larger anisotropy is seen when the DFT-based model is used. (Figure 4)

In the literature, RCB values of both monoatomic and more extended systems were computed with several methods.[5-7,10] However, to the best of our knowledge, no studies have been performed yet on the highly symmetric tetrahedral MCA's considered in this work, with the exception of SO_4^{2-}. Hydrated SO_4^{2-} was extensively studied by Yang et al.[10] Their RCB values of water-solvated SO_4^{2-} obtained with the electrostatic model varied from 2.8 to 1.2 eV, when the number of added water molecules was gradually increased from 4 to 50. These values are in excellent agreement with photon-energy-dependent PES spectra derived RCB values,[10] decreasing from 2.4 to 1.7 eV when the number of water molecules increases from 4 to 18. Using the electrostatic model, we obtain an RCB value of 3.6 eV for SO_4^{2-} in the gas phase, in agreement with the stabilization and the decrease of the RCB of MCA's in solvent. The RCB values for SO_4^{2-} obtained with the PCM and the DFT-based model in the gas phase are in line with this principle too.

The PCM model is strongly basis set dependent:[6] the RCB gradually decreases with increasing diffuseness of the basis set, hindering a direct comparison with values reported in the literature. Nevertheless, the RCB values we obtain for the tetrahedral anions are higher than those reported for monoatomic

systems such as O^{2-} and F^{2-} (refs 6 and 7). This is in accordance with chemical intuition: the larger the system, the more stable it is and thus the lower the RCB value.

Correlation between the RCB and S. The well-known trend of increasing softness when passing in analogous compounds from the second to the third row[11a,g,24] is accompanied by the decrease in the RCB values (Table 2).

For the electrostatic model, this result is expected, since from eq 2 an expression, explicitly including the charge Q of the $(N-1)$-system, of α in terms of the RCB can be written[10]

$$\alpha = \frac{629.86}{RCB^3}Q^4 \tag{12}$$

with α the polarizability of the $(N-1)$-system, given in Å^3, and the RCB given in eV. Introducing the proportionality between the polarizability α and the global softness S, put forward first by Politzer,[18] and later on derived by Vela and Gázquez,[16] one obtains from eq 12

$$S \approx RCB^{-3}Q^4 \tag{13}$$

with S the global softness of the $(n-1)$-charged system. The expected correlation was not found when S is calculated with eq 10 combined with eq 11. To overcome this, I and A of eq 10 can be approximated by respectively the energy of the Highest Occupied Molecular Orbital (ϵ_{HOMO}) and by the energy of the Lowest Unoccupied Molecular Orbital (ϵ_{LUMO}), making use of a Koopmans'[25] type of approximation yielding for S

$$S = 1/(\epsilon_{LUMO} - \epsilon_{HOMO}) \tag{14}$$

This methodology was proven before, among others by our group, to give reliable results[8,26] in applications of conceptual DFT.

When S is calculated with eq 14, a fair correlation as expected by eq 13 is now found between S and RCB^{3-} (Figure 5, $R^2 = 0.69$). The here-discussed problem illustrates the inherent difficulties of evaluating S for highly negatively charged systems.

By introducing the proposed[27] correlation between α and S^3 in eq 12, the following relationship between RCB and S^{-1} can be written

$$RCB \approx S^{-1}Q^{4/3} \tag{15}$$

Using this proportionality, a better linear correlation between the RCB and S^{-1} is found (Figure 6, $R^2 = 0.86$) arguing in favor of the proportionality between α and S^3, in agreement with Ghanty and Ghosh,[27] on the condition that eq 12 holds.

Turning to the PCM model, from eq 1, no direct evidence for a correlation between the RCB and the global softness S of the $(N-1)$-system is given. Nevertheless, the similarity between the results obtained with the PCM model and those obtained with the electrostatic model provides evidence that the inverse correlation between the RCB and S remains valid. A very good linear relationship between the RCB values of the dianionic and trianionic systems and the inverse of the global softness (calculated with eq 14) of their $(n-1)$-charged counterparts is indeed obtained (Figure 6, $R^2 = 0.93$ for dianions, $R^2 = 0.99$ for trianions). Note that because of the charge dependency of the RCB values, di- and trianionic systems are treated separately here. As a consequence, for the trianionic systems, only three points are available implying that the obtained correlation has to be treated with the necessary caution.
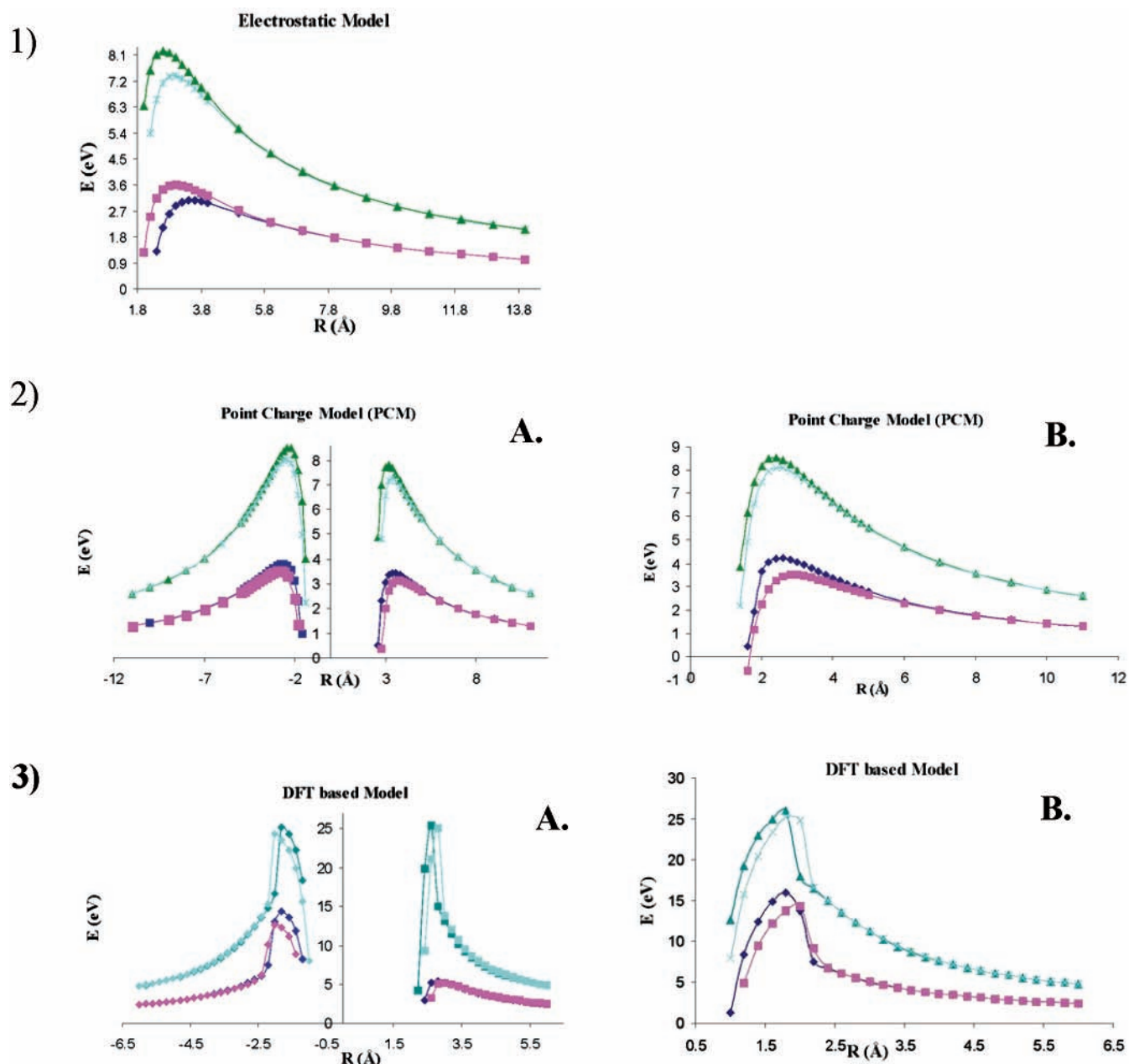
1)

2)

3)

Figure 3. Study of the RCB potentials of SO_4^{2-} (blue), SeO_4^{2-} (pink), PO_4^{3-} (green), and AsO_4^{3-} (light blue) in the gas phase obtained with (1) the electrostatic model (eq 2), (2) the PCM model (eq 1), and (3) the DFT based model (eqs 3 and 8), with S calculated with eq 10. In the case of nonspherically averaged potentials, results are given (A) along the 3-fold axis and (B) along the 2-fold axis.

Note that the discussed correlation curves are obtained for the studied anions supplied with an extra series of anionic systems (S^{2-}, O^{2-}, N^{3-}, $HAsO_4^{2-}$, and HPO_4^{2-}), to have a broader range over which the correlation can be made.

In all three approximations used in this work, the nonlocality and energy dependence is not considered. With Green's function theory, nonlocal and energy-dependent RCB's can be obtained. Exact GF results are, however, very difficult to calculate and moreover very hard to interpret with use of the softness concept. Since the relation between the RCB and the global softness of the system is the purpose of our work, we opted for a methodology involving approximations for the RCB from which a direct relationship with the global softness emerges.

Although qualitatively the results obtained with the DFT-based model are similar to those obtained with the electrostatic and the PCM models, the numerical correlation between the RCB calculated with the DFT-based model and S^{-1} is lost. The

importance of the DFT-based model can be found in the explicit presence of the global softness of the $(N - 1)$-system in the equation. Numerically, the S-dependent term dominates in eq 3. Although showing qualitative agreement, the behavior of the potential, calculated with the DFT-based model, with R deviates quantitatively from that of the potential curve calculated with the two other models (Figure 3). In the DFT-based model, the shape of the potential curve is largely dependent on the polarization term of eq 3, a local model of the softness kernel $s(\mathbf{r},\mathbf{r}')$. It is also not excluded that these discrepancies are due to the inherent difficulties of evaluating S for highly negatively charged systems. In addition, we have to mention that the relation between S and α is not exact, from which further deviations can occur.

Softness or its inverse, hardness, describes the ability to retain electronic charge once the charge has been acquired. Further, S can be approximated as the inverse of the ionization energy
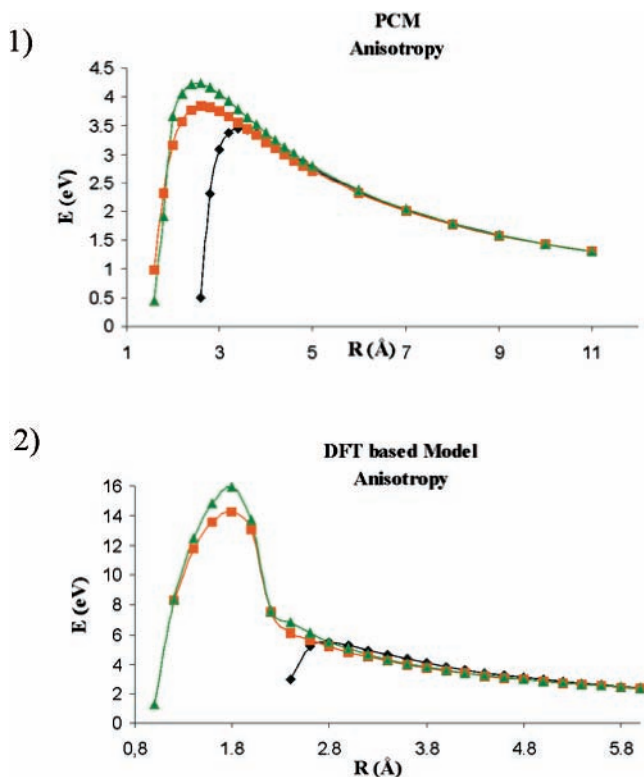
GP Stability of Tetrahedral Multiply Charged Anions

J. Phys. Chem. A, Vol. 109, No. 4, 2005 **657**

Figure 4. Anisotropy of the RCB potentials for SO_4^{2-}. The RCB values are obtained with (1) the PCM model (eq 1) and (2) the DFT based model (eqs 3 and 8), with S calculated with eq 10. Color code: twofold axis, green; threefold axis, negative direction (O−X), orange; and threefold axis, positive direction (X−O), black.
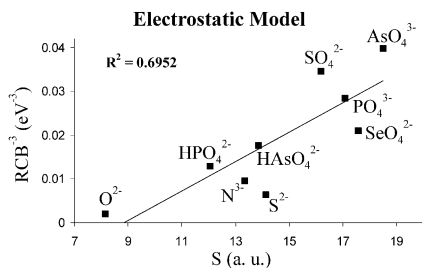

Figure 5. Correlation between S (au, calculated with eq 14) of the (n − 1) charged system and RCB^{3-} (eV^{-3}) obtained with the electrostatic model.

(when very small or negative values of the electron affinity are neglected in eq 10), which is a measure of the system's stability toward electron emission. As a consequence, through eq 3, the RCB is expressed in terms of properties describing the ease of the evolution of a system from N- to (N − 1)-electrons.

Stabilization of MCA's. The significant reduction of the RCB of solvated MCA's relative to bare ones and the continuous decrease of the RCB as more solvent is added has been described before.[10,28] In analogy to these studies, the stabilization of the prototypical MCA SO_4^{2-} in solvent is followed. Instead of adding solvent molecules in a discrete model, the dielectric constant of the continuum model is changed. RCB values are calculated with both the electrostatic model (eq 2) and the PCM model (eq 1). Both methods demonstrate a decreasing RCB when the dielectric constant increases (Figure 7), implying that the higher the dielectric constant, the more the multiply charged anion is stabilized. Although the same behavior of the RCB in the function of the dielectric constant is found for both calculation methods, the RCB decreases faster and disappears finally when the PCM model is used. The stabilization of the
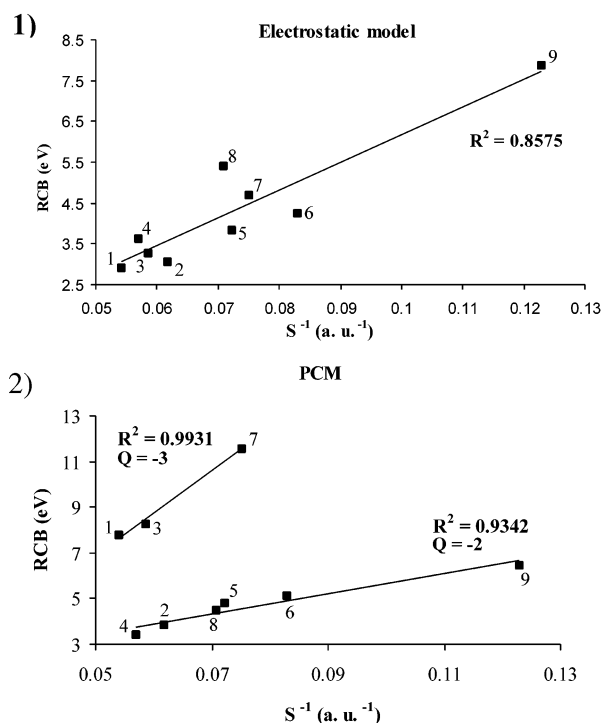

Figure 6. Correlation between the RCB (eV) calculated with (1) the electrostatic model (eq 2) and (2) the PCM model (eq 1) and S^{-1} (au^{-1}, calculated with eq 14) of the (n − 1)-charged system. Numbering of the data points: $1 = AsO_4^{3-}$, $2 = SO_4^{2-}$, $3 = PO_4^{3-}$, $4 = SeO_4^{2-}$, $5 = HAsO_4^{2-}$, $6 = HPO_4^{2-}$, $7 = N^{3-}$, $8 = S^{2-}$, and $9 = O^{2-}$.
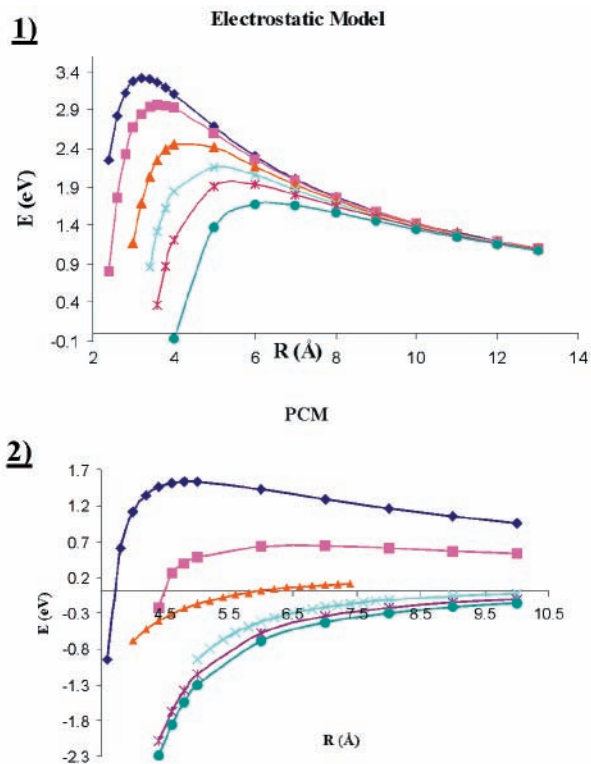

Figure 7. Study of the RCB potential of SO_4^{2-} obtained with (1) the electrostatic model (eq 2) and (2) the PCM model (eq 1) (threefold axis, X−O direction) for different values of ϵ. Color code: $\epsilon = 1.43$ (argon), blue; $\epsilon = 2.247$ (benzene), pink; $\epsilon = 4.9$ (chloroform), orange; $\epsilon = 10.36$ (dichloromethane), light blue; $\epsilon = 20.7$ (acetone), red; $\epsilon = 78.39$ (water), green.

multiply charged SO_4^{2-} in solvent is in line with the literature[10,26] and in agreement with the positive and increasing

TABLE 3: Ionization (I) and HOMO (ϵ_{HOMO}) Energies (au) and RCB Values (eV) Evaluated at the B3LYP/6-31+G Level into the Positive Direction of the Threefold X−O Axis of SO_4^{2-} with the Electrostatic (eq 2) and the PCM (eq 1) Models for Different Values of ϵ**

ϵ	I	ϵ_{HOMO}	RCB PCM	RCB electrostatic model
0	−0.048	0.132	3.847	3.627
1.43	0.035	−0.157	1.154	3.305
2.247	0.105	−0.203	0.638	2.973
4.9	0.172	−0.248	0.157	2.451
10.36	0.202	−0.267	0.041	2.158
20.7	0.215	−0.276	0.0005	1.929
78.39	0.225	−0.283	0.0001	1.675

ionization energies, and the negative and decreasing HOMO energies found when the dielectric constant of the solvent increases (Table 3).

Conclusion

RCB's have been calculated for the biologically important tetrahedral MCA's AsO_4^{3-}, PO_4^{3-}, SO_4^{2-}, and SeO_4^{2-}. Values of comparable magnitude are found with the electrostatic and the PCM models. Qualitatively, the RCB obtained with the DFT-based model displays the same pattern, but quantitatively it depends highly on the calculation of the global softness S, a property that is nontrivial to evaluate for MCA's.

The RCB values for the dianionic systems are considerably lower than those for the trianionic systems, in accordance with the strong dependence of the RCB on the electrostatic repulsion between the excess negative charge within an MCA.

An inverse correlation between the RCB and the global softness of the $(n-1)$-charged system is deduced from eq 2. A numerical relationship is found between the RCB and S^{-1} when the RCB is calculated with the electrostatic and the PCM models.

This relation is not found when the RCB values are obtained with the DFT-based model. This approach, however, has the advantage of expressing the RCB in terms of molecular reactivity descriptors, describing the evolution of a system when passing from N- to $(N-1)$-electrons and vice versa.

A decreasing RCB, implying an increasing stabilization of MCA's, is found when increasing the dielectric constant in a continuum solvent model.

References and Notes

(1) Roos, G.; Messens, J.; Loverix, S.; Wyns, L.; Geerlings, P. *J. Phys. Chem. B* **2004**, *108*, 17216.

(2) (a) Lindblow-Kull, C.; Kull, F. J.; Shrift, A. *J. Bacteriol.* **1985**, *163*, 1267. (b) Pflugrath, J. W.; Quiocho, F. A. *J. Mol. Biol.* **1988**, *200*, 163. (c) Zhang, Z.-Y. *Crit. Rev. Biochem. Mol. Biol.* **1998**, *33*, 1. (d) Bebien, M.; Kirsch, J.; Mejean, V.; Vermeglio, A. *Microbiology* **2002**, *148*, 3865.

(3) Wang, X.-B.; Nicholas, J. B.; Wang, L.-S. *J. Chem. Phys.* **2000**, *113*, 653.

(4) Skurski, P.; Simons, J.; Wang, X.-B.; Wang, L.-S. *J. Am. Chem. Soc.* **2000**, *122*, 4499.

(5) Simons, J.; Skurski, P.; Barrios, R. *J. Am. Chem. Soc.* **2000**, *122*, 11893.

(6) Dreuw, A.; Cederbaum, L. S. *Phys. Rev. A* **2000**, *63*, 049904.

(7) Dreuw, A.; Cederbaum, L. S. *Chem. Rev.* **2002**, *102*, 181.

(8) Roos, G.; Loverix, S.; De Proft, F.; Wyns, L.; Geerlings P. *J. Phys. Chem. A* **2003**, *107*, 6828.

(9) See for example: Asthagiri, D.; Dillet, V.; Liu, T.; Noodleman, L.; Van Etten, R.; Bashford, D. *J. Am. Chem. Soc.* **2002**, *124*, 10225.

(10) Yang, X.; Wang, X.-B.; Wang, L.-S. *J. Phys. Chem. A* **2002**, *106*, 7607.

(11) (a) Parr, R. G.; Yang, W. *Density-Functional Theory of Atoms and Molecules*; Oxford University Press: Oxford, 1989. (b) Parr, R. G.; Yang, W. *Annu. Rev. Phys. Chem.* **1995**, *46*, 701. (c) Geerlings, P.; De Proft, F.; Langenaeker, W. *Adv. Quantum Chem.* **1999**, *33*, 303. (d) Chermette, H. *J. Comput. Chem.* **1999**, *20*, 129. (e) Geerlings, P.; De Proft, F. *Int. J. Quantum Chem.* **2000**, *80*, 227. (f) De Proft, F.; Geerlings, P. *Chem Rev.* **2001**, *101*, 1451. (g) Geerlings, P.; De Proft, F.; Langenaeker, W. *Chem. Rev.* **2003**, *103*, 1793.

(12) Yang, W.; Parr, R. G. *Proc. Natl. Acad. Sci. U.S.A.* **1985**, *82*, 6723.

(13) Langenaeker, W.; De Proft, F.; Tielens, F.; Geerlings, P. *Chem. Phys. Lett.* **1998**, *228*, 628.

(14) Murray, J. S.; Sen, K., Ed. *Molecular Electrostatic Potentials Concepts and Applications*; Elsevier: New York, 1996.

(15) Berkowitz, M.; Parr, R. G. *J. Chem. Phys.* **1988**, *88*, 2554.

(16) Vela, A.; Gázquez, L. J. *J. Am. Chem. Soc.* **1990**, *112*, 1490.

(17) (a) Cohen, M. H.; Ganduglia-Pirovano, M. V.; Kudrnovsky, J. *J. Chem. Phys.* **1994**, *101*, 8988. (b) Cohen, M. H.; Ganduglia-Pirovano, M. V.; Kudrnovsky, J. *J. Chem. Phys.* **1995**, *103*, 3543. (c) Geerlings, P.; De Proft, F.; Balawender, R. *Reviews of Modern Quantum Chemistry, A Celebration to the Contributions of R. G. Parr*; Sen, K. D., Ed.; World Scientific: Singapore, 2002; pp1053−1070.

(18) Politzer P. *J. Chem. Phys.* **1987**, *86*, 1072.

(19) (a) Lee, C.; Yang, W.; Parr, R. G. *Phys. Rev.* **1998**, *37*, 2. (b) Becke, A. D. J. *Chem. Phys.* **1993**, *98*, 5648.

(20) For a detailed account of this type of basis set see, for example: Hehre, W.; Radom, L.; Schleyer, P. v. R.; Pople, J. A. *Ab Initio Molecular Orbital Theory*; Wiley: New York, 1986.

(21) (a) Wiberg, K. B.; Keith, T. A.; Frisch, M. J.; Murcko, M. *J. Phys. Chem.* **1995**, *99*, 9072. (b) Foresman, J. B.; Keith, T. A.; Wiberg, K. B.; Snoonian, J.; Frisch, M. J. *J. Phys. Chem.* **1996**, *100*, 16096. (c) Foresman, J. B.; Frisch, M. J. *Exploring Chemistry with Electronic Structure Methods*, 2nd ed.; Gaussian, Inc: Pitsburgh, PA, 1996. (d) Safi, B.; Choho, K.; De Proft, F.; Geerlings, P. *J. Phys. Chem.* **1998**, *102*, 5253.

(22) Frisch, M. J.; Trucks, G. W.; Schlegel, H. B.; Scuseria, G. E.; Robb, M. A.; Cheeseman, J. R.; Montgomery, J. A., Jr.; Vreven, T.; Kudin, K. N.; Burant, J. C.; Millam, J. M.; Iyengar, S. S.; Tomasi, J.; Barone, V.; Mennucci, B.; Cossi, M.; Scalmani, G.; Rega, N.; Petersson, G. A.; Nakatsuji, H.; Hada, M.; Ehara, M.; Toyota, K.; Fukuda, R.; Hasegawa, J.; Ishida, M.; Nakajima, T.; Honda, Y.; Kitao, O.; Nakai, H.; Klene, M.; Li, X.; Knox, J. E.; Hratchian, H. P.; Cross, J. B.; Adamo, C.; Jaramillo, J.; Gomperts, R.; Stratmann, R. E.; Yazyev, O.; Austin, A. J.; Cammi, R.; Pomelli, C.; Ochterski, J. W.; Ayala, P. Y.; Morokuma, K.; Voth, G. A.; Salvador, P.; Dannenberg, J. J.; Zakrzewski, V. G.; Dapprich, S.; Daniels, A. D.; Strain, M. C.; Farkas, O.; Malick, D. K.; Rabuck, A. D.; Raghavachari, K.; Foresman, J. B.; Ortiz, J. V.; Cui, Q.; Baboul, A. G.; Clifford, S.; Cioslowski, J.; Stefanov, B. B.; Liu, G.; Liashenko, A.; Piskorz, P.; Komaromi, I.; Martin, R. L.; Fox, D. J.; Keith, T.; Al-Laham, M. A.; Peng, C. Y.; Nanayakkara, A.; Challacombe, M.; Gill, P. M. W.; Johnson, B.; Chen, W.; Wong, M. W.; Gonzalez, C.; Pople, J. A. *Gaussian 03*, revision B.01; Gaussian, Inc.: Pittsburgh, PA, 2003.

(23) Boldyrev, A. I.; Simons, J. *J. Phys. Chem.* **1994**, *98*, 2298.

(24) De Proft, F.; Langenaeker, W.; Geerlings, P. *J. Phys. Chem.* **1993**, *97*, 1826.

(25) Koopmans T. A. *Physica* **1933**, *1*, 104.

(26) Nguyen, L. T.; De Proft, F.; Casas Amat, M.; Van Lier G.; Fowler, P. W.; Geerlings, P. *J. Phys. Chem. A* **2003**, *107*, 6837.

(27) (a) Ghanty, T. K.; Ghosh, S. K. *J. Phys. Chem.* **1993**, *97*, 4951. (b) Nagle, J. K. *J. Am. Chem. Soc.* **1990**, *112*, 1490.

(28) Stefanovich, E. V.; Boldyrev, A. I.; Truong, T. N.; Simons, J. *J. Phys. Chem. B* **1998**, *102*, 4205.